Simple Brillouin-zone scheme for the spectral properties of solids*

An-Ban Chen
Department of Physics, Auburn University, Auburn, Alabama 36830
(Received 16 May 1977)

This work is a result of search for an efficient and accurate scheme for the calculation of solid-state properties from the k-space integration inside the Brillouin zone (BZ). A survey shows that because of the lack of a satisfactory interpolation method the presently available BZ schemes are either too complicated or too specialized to be desired for accurate and vast applications. A scheme which uses a small number of first-principles k points (~ 150) to achieve a high accuracy has been obtained. The special feature of the scheme is the utilization of a set of coordinates which allow the interpolation and integration to be carried out in a systematic one-dimensional manner. The problem associated with the band crossing and band switching in real crystals can also be handled easily within the scheme. The quality of the scheme has been satisfactorily tested by a direct comparison of the calculated density of states with the exact results for the tight-binding band models. The electronic density of states for Cu has also been calculated to demonstrate the applicability of the scheme in real crystals. With its simplicity, generality, and accuracy, the present scheme should be very useful for the calculation of various spectral properties of solids. The application of this scheme in the study of impurities and disordered alloys and in connection with the empirical parametrization of the electronic structure of solids is also discussed.

I. INTRODUCTION

The importance of the techniques of k-space interpolation and integration in the Brillouin zone[1-3] (BZ) has been well recognized in the field of band-structure calculation. Besides being an indispensable part in many important calculations such as the self-consistent band calculations and Green's-function formalisms for the impurities in crystals[4-5] and for the disordered alloys,[6-13] the BZ integration is the basic tool for the band calculation of various solid-state properties such as density of states, optical spectra, charge densities, photoelectric spectra, and susceptibility functions, etc. More theorists and experimentalists now than before seem to be more interested in these calculations. Although many sophisticated BZ schemes are available, we find, from the survey to follow, that there is no simple scheme which has the desired uniformity and efficiency for vast and accurate calculations. The search for such a scheme motivated the present work.

Another motivation for the present work is its connection with the application of a parametrization scheme for the electronic structure based on Green's-function method[14] (GFM) of Korringa, Kohn, and Rostoker (KKR)[15,16] recently developed by Chen and Segall.[17] That scheme provides an effective means for modifying the *ab initio* potentials to yield energy bands $E_n(\vec{k})$ in agreement with the experimental data. Means for obtaining the wave functions $\Psi_n(\vec{k})$ and related quantities from the parametrized quantities has also been implemented.[18] In order to apply the parametrization scheme more effectively, it is necessary to have a good BZ scheme which serves not only to relate the parametrized $E_n(\vec{k})$ and $\Psi_n(\vec{k})$ directly to the experiments but also to extract band parameters from the data. It is believed that that parametrization scheme, when coupled with the BZ scheme developed in this paper, would become a very useful tool for the quantitative study of the electronic structures in crystals.

Most of the properties mentioned above can be represented by a general spectral function,

$$F(\omega^+) = R(\omega) - i\pi I(\omega) \equiv \int_{\mathrm{BZ}} d^3k \, \frac{f(\vec{k})}{(\omega^+ - \omega(\vec{k}))} , \qquad (1)$$

where the energy parameter $\omega^+ \equiv \omega + i0$ contains an infinitesimal positive imaginary part, $f(\vec{k})$ is a function of $E_n(\vec{k})$ and the matrix elements $M(\vec{k})$, and $\omega(\vec{k})$ is either the $E_n(\vec{k})$ or the difference in band energies. The integration in Eq. (1), by symmetry, can be reduced to that in a smaller volume so-called the irreducible wedges of the BZ (IBZ). While the real part $R(\omega)$ and the imaginary part $I(\omega)$ of Eq. (1) can be related to each other by dispersion relations, the functions which are calculated more often are the $I(\omega)$,

$$I(\omega) = \int_{\mathrm{BZ}} d^3k f(\vec{k}) \delta(\omega - \omega(\vec{k})) , \qquad (2)$$

and the integrated function

$$J(\omega) \equiv \int_{-\infty}^{\omega} d\omega' I(\omega') = \int_{\mathrm{BZ}, \omega(k) \le \omega} d^3k f(\vec{k}) . \qquad (3)$$

An accurate numerical evaluation of these integrals usually requires the use of very fine mesh, say 10^4 $\vec{k}$ points or more. However, because the calculation of $E_n(\vec{k})$ and $M(\vec{k})$, particularly for electrons,

normally involves large matrices and lengthy numerical procedures, a direct calculation of these band quantities on such fine mesh is considered impractical. What is usually done is to calculate the $E_n(\vec{k})$ and $M(\vec{k})$ on a coarse first-principles grid containing, say, N_k points in the IBZ and then to interpolate them on a finer mesh. The difficulties in the BZ interpolations have arisen primarily from the piece-wise continuous nature of the bands and from the nonrectangular geometry of the BZ. The constraint on the integration space imposed by the IBZ and the singular behavior of the integrand cause further difficulties. Thus, special numerical techniques are required for the BZ integration and interpolation.

Considerable work has been done for the BZ integration in the past and many sophisticated schemes are now available. The main schemes include (i) the root sampling method[19,20]; (ii) the linear discrete method[21]; (iii) the linear analytic method[22,23]; (iv) the quadratic (QUAD) scheme[24,25]; (v) the hybrid methods[26,27]; and (vi) the tetrahedron scheme.[28,29] A comprehensive comparison of the first five schemes can be found in the review papers by Gilat.[2,3] The tetrahedron scheme has also been discussed in some detail by Rath and Freeman.[28] A critical comparison between the two popular methods (iii) and (iv) was made by Gilat and Herman.[30] Although the computational details are different for different schemes, the integration techniques used can generally be characterized as being either the sampling of $\vec{k}$ points in the IBZ or the summation over many microzones in which the integrations are carried out analytically in a linear or quadratic approximation. It is perhaps fair to say that all these integration schemes can give accurate results if sufficiently fine mesh is used and accurate band quantities on the mesh are available. Therefore, the problem of BZ integration is really not in the integration itself but lies in the problem of obtaining accurate band quantities on the mesh—i.e., the problem of BZ interpolation.

The main interpolation methods employed in the past can be represented by three approaches: (a) the three-dimensional numerical interpolation,[23-25] (b) the model Hamiltonian interpolation scheme,[31-35] and (c) the local $\vec{k}\cdot\vec{p}$ method.[36] The first method has been limited to the linear and quadratic interpolations since the number of terms increases drastically fast with the order of interpolation. Treating the band crossing[23] is a major problem in this approach. To achieve adequate accuracy, a large number of first-principles $\vec{k}$ points, N_k, ($N_k \gtrsim 10^3$) is needed. In the model Hamiltonian approach, the parameters required for the Hamiltonian matrix elements are determined from fitting the band energies at selected $\vec{k}$ points and the resultant Hamiltonian matrix is then used to generate band energies on the integration mesh. There is no problem for this method to deal with the band crossing and band switching and the N_k needed is not large. Although a model Hamiltonian can be made to yield bands appropriate for certain spectra like the photoemission, there is a basic question about its capability in pinning down the energy accurately (say, to 10^{-3} Ry). Yet the major objection to this method is in its lack of uniformity, namely, different Hamiltonians are needed for different types of bands or even for different energy ranges of the same band structure. For example, a 4×4 orthogonalized-plane-wave (OPW) model Hamiltonian, which may work well for the lower energy bands for Al, is certainly not good for a d-band metal or for the higher energy bands for Al. Moreover, the diagonalization of the model Hamiltonian on the fine mesh can be very time consuming. There is also a question about obtaining the wave functions and the related quantities from this method. The local $\vec{k}\cdot\vec{p}$ method represents a combination of the above two approaches. In this approach the band energies (and energy gradients) are extrapolated from the closest first-principles k point using the $\vec{k}\cdot\vec{p}$ Hamiltonian. In order to apply this method, several bands above the energy range of interest have to be included. Since only a finite number of bands are included in the calculation, the accuracy is not uniform throughout the energy range. To achieve accuracy, a large N_k is also needed. This method may also produce spurious discontinuities in the bands.[36]

Thus from the above and from the discussion in Sec. VI, we conclude that, because of the lack of a good interpolation scheme, the presently available BZ integration schemes are still too complicated or too specialized to be desired for accurate and vast calculations. However, since the above schemes have been developed to a high level of sophistication, it is very difficult to make a significant improvement without considering a new approach. The most desired improvements, in our opinion, would be the development of a general numerical interpolation scheme which uses a small N_k to achieve the desired accuracy.

In Sec. II we show that the BZ interpolation can be carried out accurately and efficiently using systematic one-dimensional procedures based on a system of coordinates which conveniently define the geometry of an IBZ.

In Sec. III, two BZ integration methods which are compatible with the interpolation scheme are investigated. The first method is a direct numerical integration and the second method divides the IBZ into a bundle of thin wedges (TW). The angular

dependence of the integrand in each TW is treated as constant so that only one-dimensional integrations along the axes of the TW are needed—a ray integration. Both methods have been tested on the single tight-binding band models for the sc, bcc, and fcc crystals and the results are presented in Sec. IV. There the calculated density of states $g(E)$ and the integrated density of states $\Phi(E)$ are compared with the exact results.[37] With a $N_k \sim 150$, the scheme has achieved the desired accuracy: $E(\vec{k})$ is accurate to 0.001 of the band width and the accuracies of the averaged $|\Delta g/g|$ and $|\Delta\Phi/\Phi|$ are found to be 0.5% and 0.1%, respectively. Some numerical results from previous schemes are also quoted for comparison.

The ray integration turns out to be more accurate and more useful, particularly in the application in real crystals. In Sec. V, we show that the band crossing and band switching can be handled easily within the ray scheme. The density of states for a Cu electronic band structure has also been calculated to demonstrate the applicability of the scheme in real crystals. The final section (Sec. VI) contains a summary and discussion, where the present approach is related to the previous schemes and a brief discussion is made of the application of the scheme in the study of impurities and disordered alloys.

II. COORDINATES AND INTERPOLATION

Since all the IBZ of the symmorphic space group[38] can be decomposed into one or several tetrahedrons or triangular prisms, in practice, we only need to consider these two geometries. Below we shall discuss the case of the tetrahedron only. The results can be readily extended to the other case.

Consider the tetrahedron ΓABC shown in Fig. 1. Γ is the center of the BZ and ABC is part of the zone surface. First, we note that any $\vec{k}$ vector (ΓP) inside ΓABC can be expressed in terms of the three basis vectors $\vec{q}_1$ (ΓA), $\vec{q}_2$ (AB), and $\vec{q}_3$ (BC):

$$\vec{k} = \alpha\vec{q}_1 + \alpha\beta\vec{q}_2 + \alpha\beta\gamma\vec{q}_3, \tag{4}$$

where α is the $\Gamma A'/\Gamma A$, β is $A'L/A'B'$, and $\gamma = LP/LM$ shown in Fig. 1. The values of α, β, and γ defined above all range from 0 to 1. In fact, these three parameters define three sets of independent planes: All the $\vec{k}$ points with the same α lie on a plane parallel to ABC; a given β defines a plane parallel to ΓBC; and γ represents those planes starting with ΓAB and ending with ΓAC. The end point of a $\vec{k}$ vector defined by Eq. (4) (i.e., P in Fig. 1) corresponds to the point where the three planes, respectively, corresponding to α, β, and γ intersect. Thus the (α,β,γ) form a convenient set of coordinates for the k space inside the tetrahedron.

One advantage of using these coordinates is that the BZ interpolation can be cast into systematic one-dimensional procedures. In order to simplify the presentation, we shall consider a single band first. The application to the multiple bands in real crystals will be delayed to Sec. V. Let us start by considering the interpolation along a line, say ΓA in Fig. 1. We observe that the energies $E(\alpha)$ of a smooth band along ΓA can be interpolated accurately from several calculated $E(\alpha_i)$ on a reasonable grid $\{\alpha_i\}$ with a reasonable interpolation method (e.g., the Lagrange's formula), i.e.,

$$E(\alpha) = \sum_i L_i(\alpha)\, E(\alpha_i), \tag{5}$$

where $L_i(\alpha)$ are the interpolation coefficients and the number of α_i in the summation depends on the order of the interpolation rule. To generalize Eq. (5) to any $\vec{k}$ point inside the ΓABC, say (α,β,γ), we need to calculate the $E(\vec{k})$ at a set of grid points $\{\alpha_i,\beta_j,\gamma_m\}$ with i from 1 to N_A, j from 1 to N_B, and m from 1 to N_C and with $\alpha_1 = \beta_1 = \gamma_1 = 0$ and $\alpha_{N_A} = \beta_{N_B} = \gamma_{N_C} = 1$. Then $E(\alpha,\beta,\gamma)$ can be obtained from the triple one-dimensional interpolations:

$$E(\alpha,\beta,\gamma) = \sum_i \sum_j \sum_m L_i(\alpha)\, L_j(\beta)\, L_m(\gamma)\, E(\alpha_i,\beta_j,\gamma_m). \tag{6}$$

Again, the numbers of terms in the summations depend on the orders of interpolation schemes used.

We note that the interpolation coefficients $L_i(\alpha)$, $L_j(\beta)$, and $L_m(\gamma)$ in Eq. (6) are independent of each other and with a proper choice of the mesh and the order of interpolations they can be repeatedly used in the process of integration. For example, the same set of $\{L_i(\alpha)\}$ can be used for all the k points on the same plane with the same α. The same situations hold for $\{L_j(\beta)\}$ and $\{L_m(\gamma)\}$. In practice,

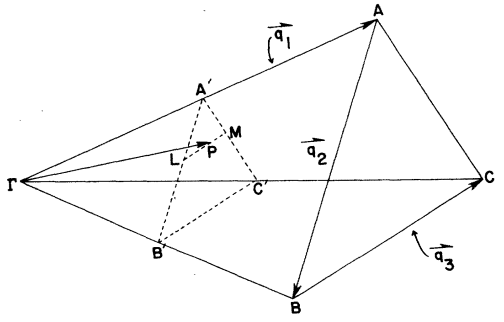

FIG. 1. Any vector ΓP inside the tetrahedron ΓABC can be conveniently expressed in terms of $\vec{q}_1$, $\vec{q}_2$, and $\vec{q}_3$ and the three normalized coordinates (α,β,γ) defined in Eq. (4).

high-order interpolations can be carried out with great efficiency.

Another advantage of using these coordinates is that the normalizations (α, β, and γ all range from 0 to 1) make it easy to set up integration mesh and the interpolation grid and thus simplify the computer coding. Finally, using these coordinates, the interpolation in Eq. (6) is never across any symmetry plane or any symmetry axis so that the band crossing and band switching in real crystals (see Sec. V) can be avoided and a smooth interpolation using Eq. (6) is always possible.

III. INTEGRATION SCHEMES

A. Direct integration

The direct integration is a brute-force numerical evaluation of Eq. (3), which can be rewritten as

$$J(\omega) = \int_{\mathrm{IBZ}, \omega(\vec{k}) \le \omega} dh \int ds f(\vec{k}), \tag{7}$$

where s is the surface of the triangle $A'B'C'$ (see Fig. 1) and the h measures the vertical distance from Γ to s. The surface integral can be decomposed into line integrals

$$\int ds f(\vec{k}) = \iint dw\, dt f(\vec{k}), \tag{8}$$

where w is the distance from A' to LM and $t = LP$. If the vertical distance from Γ to the plane ABC is H, that from A to BC is W and the length of the BC line is T; then $h = \alpha H$, $w = \alpha\beta W$, $t = \alpha\beta\gamma T$, and $HWT = 6V$ with V the volume of the tetrahedron ΓABC. Eq. (7) finally becomes

$$J(\omega) = 6V \int_0^1 d\alpha \int_0^1 d\beta \int_{0, \omega(\alpha,\beta,\gamma) \le \omega}^1 d\gamma\, \alpha^2 \beta f(\alpha, \beta, \gamma). \tag{9}$$

Eq. (6) can now be applied effectively in Eq. (9). The summation over the α_i provides the energies on the interpolation grid on the surface specified by α. The summation over the β_j then gives the $E(\vec{k})$ on the interpolation grid along the line LPM. The line integral over γ can now be evaluated numerically. Following the line integral, the integrations over β and then α can be carried out using one-dimensional numerical procedures. We note that the fact that integration limits for α, β and γ all range from 0 to 1 has essentially transformed the geometry of the tetrahedron into that of a cube.

We should point out that although Eq. (2) can be cast into a similar expression

$$I(\omega) = 6V \int_0^1 d\alpha\, \alpha^2 \int_0^1 d\beta\, \beta \int_0^1 d\gamma f(\alpha, \beta, \gamma) \times \delta(\omega - \omega(\alpha, \beta, \gamma)), \tag{10}$$

caution must be exercised in the numerical integrations for β and α which involve piece-wise functions in the integrands.

B. Ray integration

Here we consider a second and more useful integration method. This approach divides the tetrahedron into a bundle of thin tetrahedrons (TT). This can be done simply by dividing the triangle ABC into smaller ones as schematically shown in Fig. 2. The integration of $I(\omega)$ can be expressed as the sum of those in the TT's

$$I(\omega) = \sum_i I_i(\omega) \equiv \sum_i \int d\Omega_i\, dk\, k^2 f(\vec{k})\, \delta(\omega - \omega(\vec{k})). \tag{11}$$

If the TT is thin enough, the angular dependence can be approximated as constant and $I_i(\omega)$ becomes

$$I_i(\omega) \simeq \Delta\Omega_i \int dk_i\, k_i^2 f(k_i)\, \delta(\omega - \omega(k_i)) = \Delta\Omega_i \sum_r f(k_r) k_r^2 \left(\left| \frac{d\omega(k_i)}{dk_i} \right|_{k_i = k_r} \right)^{-1}, \tag{12}$$

where $\Delta\Omega_i$ is the solid angle element of the TT, k_i is along the axis of the TT and the summation includes all the roots k_r satisfying $\omega - \omega(k_r) = 0$ along the axis. The k_i can be related to α by $k_i = \alpha k_t$ with k_t the length of the axis. Then $\Delta\Omega_i$ becomes $\Delta\vec{S}_i \cdot \vec{k}_t / k_t^3 = 3V(\Delta s_i/s)/k_t^3 \equiv 3V\delta_i/k_t^3$, where V is the volume of ΓABC and $\delta_i \equiv \Delta s_i / s$ with Δs_i the area at the end of the TT and s the area of ABC. Thus $I_i(\omega)$ becomes

$$I_i(\omega) = 3V\delta_i \sum_r f(\alpha_r) \alpha_r^2 \left(\left| \frac{d\omega(\alpha)}{d\alpha} \right|_{\alpha = \alpha_r} \right)^{-1}. \tag{13}$$

Similarly, the $J(\omega)$ becomes

$$J(\omega) = 3V \sum_i \delta_i \int_{\omega(\alpha_i) \le \omega} d\alpha_i\, \alpha_i^2 f(\alpha_i). \tag{14}$$

Thus the BZ integrations are replaced by those one-dimensional ones along the bundle of rays (the axes of the TT). We shall refer to this meth-

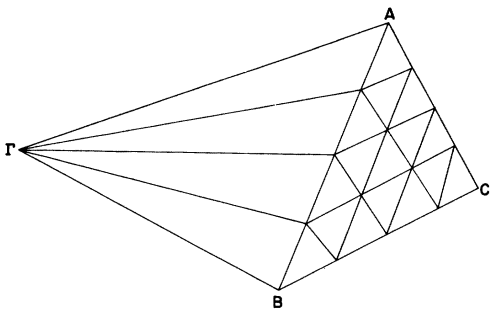

FIG. 2. A simple way to divide ΓABC into thin tetrahedrons is to divide ABC into small triangles.

od as the "ray integration." We note that the roots, the derivatives, and the integrations can all be obtained accurately with one-dimensional numerical procedures. As will be clear later, this ray integration turns out to be a more effective method in the real application.

IV. TEST AND COMPARISON

To test the applicability of the methods developed in Secs. II and III, we have tried them on the single tight-binding band models for which the exact density of states $g(E)$[37] are available for comparison. The band energies for the sc, bcc, and fcc are, respectively, given by Eqs. (17a), (17b), and (17c) below:

$$E(\vec{k}) = -\cos(k_x a) - \cos(k_y a) - \cos(k_z a)\,, \tag{17a}$$

$$E(\vec{k}) = -\cos(\tfrac{1}{2}k_x a)\cos(\tfrac{1}{2}k_y a)\cos(\tfrac{1}{2}k_z a)\,, \tag{17b}$$

$$E(\vec{k}) = -\cos(\tfrac{1}{2}k_x a)\cos(\tfrac{1}{2}k_y a) - \cos(\tfrac{1}{2}k_y a)\cos(\tfrac{1}{2}k_z a) - \cos(\tfrac{1}{2}k_z a)\cos(\tfrac{1}{2}k_x a)\,, \tag{17c}$$

where a is the lattice constant.

The IBZ for the sc (i.e., ΓXMR) and for the bcc (i.e., ΓPNH) are themselves tetrahedrons and the IBZ of fcc contains three irreducible tetrahedrons (i.e., ΓXWU, ΓLWU, and ΓLWK). The expressions for the $g(E)$ and for the integrated density of states $\Phi(E)$ which have the same normalizations as those used by Jelitto[37] are those corresponding to Eqs. (9), (13), and (14) with the function f set equal to a constant factor a^3. The members which determine the N_k value are the set (N_A, N_B, N_C) which define the interpolation grid. For simplicity, the set (N_A, N_B, N_C) will also be used as the number of points in the interpolation formulas for α, β, and γ, respectively. Also, Lagrange's formula for the interpolation and Bode's[39] rule for the integration will be used.

Table I shows the deviations in the interpolated energies ΔE normalized to the band width W for three selected sets of (N_A, N_B, N_C). The corresponding values for the N_k are also listed. The results are based on a sample of 1000 $\vec{k}$ points in each tetrahedron. We see that the average absolute deviations $\langle|\Delta E/W|\rangle$ for all cases are less than 10^{-4} and the maximum deviation $|\Delta E/W|_{\max}$ is about 3×10^{-3}. To get an accuracy corresponding to a maximum $\Delta E/W$ of 10^{-3}, a $N_k \simeq 150$ (i.e., $N_A = N_B = N_C = 6$ for sc and bcc and $N_A = 6, N_B = N_C = 4$ for fcc) is needed for all the three lattice structures.

The $g(E)$ and $\Phi(E)$ have also been calculated for the three sets of (N_A, N_B, N_C) listed in Table I. The fine mesh in the direct integration is equivalent to dividing q_1, q_2, and q_3 of Fig. 1 into 100 equally spaced meshes. The $E(\vec{k})$ on the fine mesh were interpolated using Eq. (6). As mentioned earlier, the direct integration for the $I(\omega)$ [or the $g(E)$] which involves piece-wise functions is not expected to be as reliable as the $J(\omega)$ [or the $\Phi(E)$]. Therefore, in the application of the direct integration, the $\Phi(E)$ was calculated from Eq. (9) first and then the $g(E)$ was obtained from the numerical differentiation:

$$g(E_i) = [\Phi(E_{i+1}) - \Phi(E_{i-1})]/(E_{i+1} - E_{i-1})\,.$$

Figures 3 and 4, respectively, show the comparisons of the $\Phi(E)$ and $g(E)$ calculated in this manner with the exact results.[40] In each figure, the solid curves are the exact results and the circles are the calculated values. The (N_A, N_B, N_C) used are indicated in the figure captions. The integrated $\Phi(E)$ are seen to fall on the solid curves without apparent deviations. The resultant $g(E)$ shows very little noise and fall well on the exact curves except at energies close to Van Hove's singularities where small deviations are detectable. A comparison of Fig. 4(a) with a plot[41] in Ref. 2 for the results based on the same band model from other schemes shows that the quality of our calculations is at least as good as the best results presented there.

The $g(E)$ and $\Phi(E)$ have also been calculated directly from Eqs. (13) and (14) for the ray scheme. In the calculation, each irreducible tetrahedron was divided into 40×40 thin wedges in a manner sketched in Fig. 2. Each ray is further divided into 50 fine meshes for the integration. The roots α_r needed for both Eqs. (13) and (14) were obtained by fitting three successive fine meshes to a quadratic function. The resultant $g(E)$ and $\Phi(E)$, when plotted, look essentially the same as those from the direct scheme shown in Figs. 3 and 4. But a detailed quantitative comparison below shows that the ray scheme gives even better results.

Table II lists the average absolute percentage deviations based on the energy points shown in Figs. 3 and 4. All the $\langle|\Delta\Phi/\Phi|\rangle$ tabulated are less than 0.5%. For a $N_k \sim 150$, the $\langle|\Delta\Phi/\Phi|\rangle$ can be reduced to 0.1% for the sc, bcc, and fcc. Thus, it

TABLE I. The maximum deviations $10^5\,|\Delta E/W|_{\max}$ and the average absolute deviations $10^5\,\langle|\Delta E/W|\rangle$ of the interpolated energies normalized to the band width W for a sample of 1000 k points in each irreducible tetrahedron for three sets of interpolation grids.

N_A	N_B	N_C	N_k sc	N_k bcc	N_k fcc	$10^5\|\Delta E/W\|_{\max}$ sc	$10^5\|\Delta E/W\|_{\max}$ bcc	$10^5\|\Delta E/W\|_{\max}$ fcc	$10^5\langle|\Delta E/W|\rangle$ sc	$10^5\langle|\Delta E/W|\rangle$ bcc	$10^5\langle|\Delta E/W|\rangle$ fcc
6	4	4	66	66	147	213	205	149	5	8	4
6	5	5	106	106	250	134	312	110	2	4	3
6	6	6	166	166	391	9	9	112	<1	<1	3

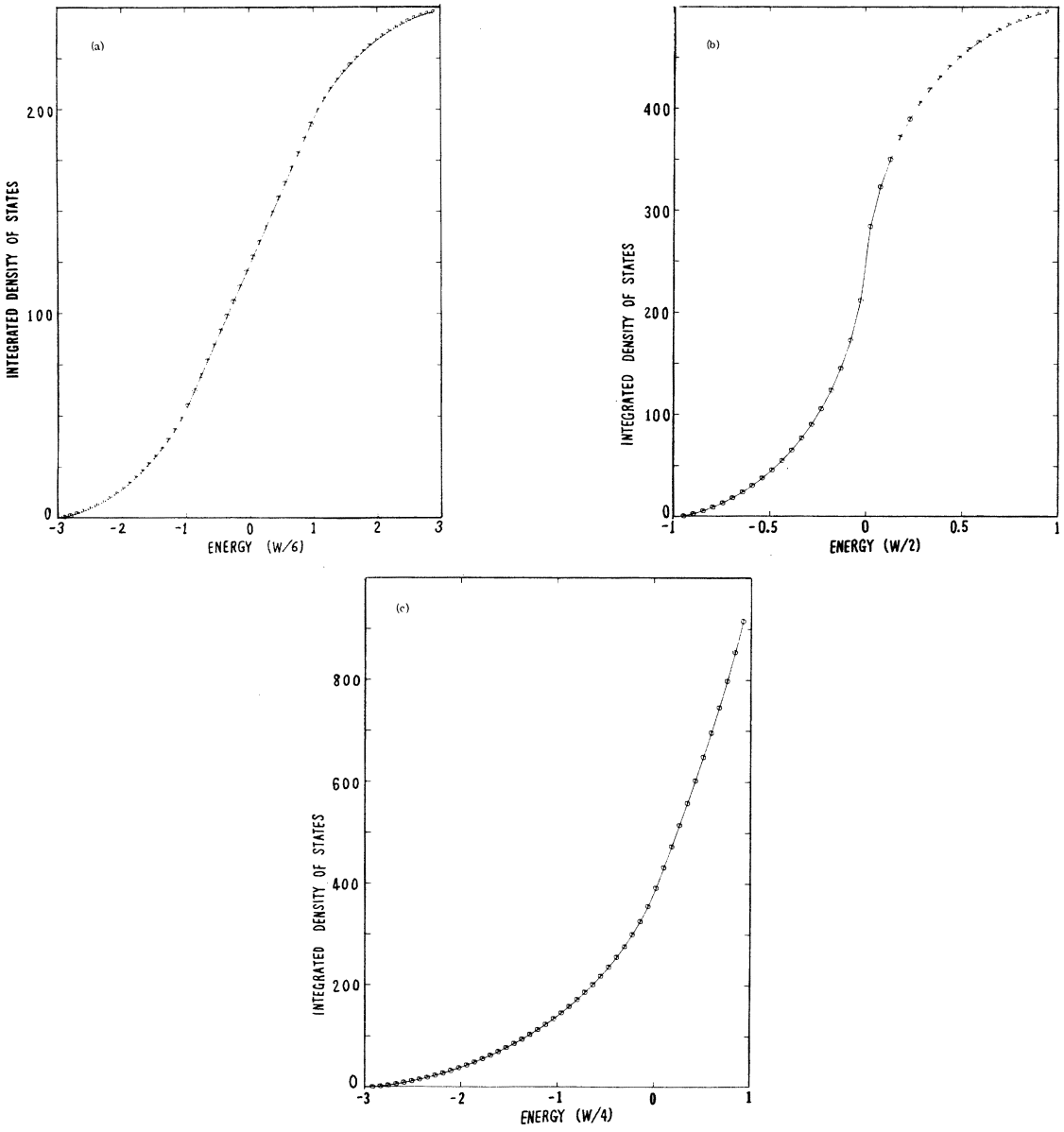

FIG. 3. Integrated density of states $\Phi(E)$ (arbitrary units) as a function of energy (in fractions of band width W) for the tight-binding bands given in Eq. (17) for the three lattice structures. The solid curves are the exact results (Ref. 40) and the circles are the calculated values from the direct scheme as described in the text. (a) and (b) are the results for sc and bcc, respectively, with $N_A = N_B = N_C = 6$, and (c) is for the fcc with $N_A = 6$ and $N_B = N_C = 4$.

is clear that the $\Phi(E)$ can be computed accurately and easily from our scheme. For the $g(E)$, we see that the Δg for sc and bcc are larger and more sensitive to the different N_k used than those for the fcc. The deviations from the ray integration are in general smaller than those from the direct scheme. With a $N_k \sim 150$, the ray integration can bring the $\langle|\Delta g/g|\rangle$ down to ~0.5% for all the three crystal structures.

Since we are not in a position to compare the above results directly with other schemes, it is useful to quote some published results for the numerical tests on other schemes for a qualitative comparison. Janak *et al.*[42] found that a 27-point three-dimensional Lagrange interpolation with a $N_k = 3345$ gave an rms deviation of 5×10^{-4} Ry and a maximum error $\Delta E_{\max}$ of 5×10^{-3} Ry for the energy bands of Pd. The maximum error became as

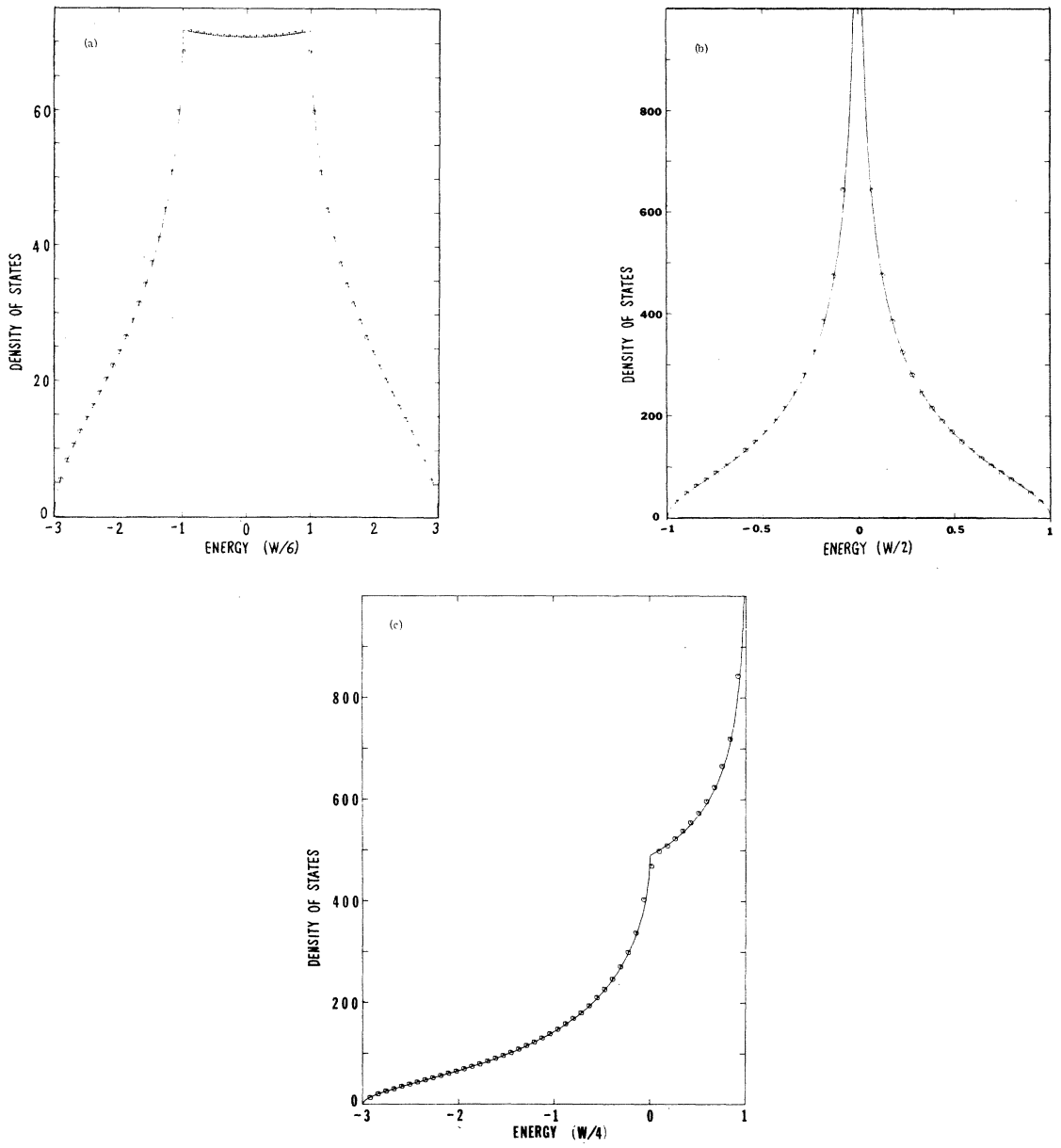

FIG. 4. Density of states $g(E)$ (arbitrary units) as a function of energy (in fractions of band width W) for the tight-binding bands given in Eq. (17) for the three lattice structures. The solid curves are the exact results (Ref. 37) and the circles are the calculated values from the direct scheme as described in the text. (a) and (b) are the results for sc and bcc, respectively, with $N_A=N_B=N_C=6$, and (c) is for fcc with $N_A=6$ and $N_B=N_C=4$.

large as 0.05 Ry with a N_k value of 89. To get the maximum error to 0.01 Ry a $N_k \sim 1000$ was needed.[23] Hodges *et al.*[31] used a 9×9 model Hamiltonian with 14 parameters for Cu and found an rms ΔE of 0.008 Ry and a $\Delta E_{\max}$ from 0.025 Ry while Mueller[32] used a slightly different version with 11 parameters and obtained an rms ΔE of 0.006 Ry and a $\Delta E_{\max}$ = 0.013 Ry. In a systematic parametrization of $E_n(\vec{k})$ for the noble and transition metals up to high energies (12 eV above E_F), Smith and Mattheiss[35] found the rms ΔE varying from 0.0035 to 0.0186 Ry and $\Delta E_{\max}$ from 0.012 to 0.077 Ry. Connolly,[33] who used a 9×9 tight-binding Hamiltonian with 27 parameters in a nonlinear fitting of the Cu and Fe bands, was able to achieve an rms $\Delta E \sim 0.003$ Ry and a $\Delta E_{\max} \sim 0.01$ Ry. For the integration, Ken-

nard *et al.*[43] tested the QUAD scheme on the parabolic band in fcc. With a $N_k = 1024$, they obtained deviations of 9.84%, 5.59%, and 3.56% in the density of states from an integration mesh of 5000, 25000, and 100000 k points in the BZ, respectively. Regarding the convergence at Van Hove's singularities, Janak[23] tested the Gilat-Raubenheimer[22] scheme on the density of states for a 2-OPW band structure around the symmetry point L and pointed out that the error still exceeded 1% even with a N_k as large as 10000.

Finally, we note that the tetrahedron scheme recently has been applied successfully to the susceptibility function $\chi(\vec{q}, \omega)$ for the electrons in crystals.[28,29] Rath and Freeman[28] have tested the accuracy of the scheme by calculating the Lindhard function $\chi(\vec{q}, \omega = 0)$ in the sc crystal. They found that maximum errors of 2.5% and 1.5% and average errors of 1.25% and 0.75% resulted from using meshes corresponding to dividing the ΓX into 12 and 16 equal spaces, respectively. The same test in the hcp crystal has also been made by Lingård.[29] Using meshes with 1152, 9216, and 31104 $\vec{k}$ points in the BZ, he found that the errors for the χ at $q = 2k_F$ were 15%, 9%, and 2.2% respectively. More relevant for comparison with our results are the corresponding volume deficiencies (i.e., $\Delta\Phi/\Phi$) quoted by Lingård, which were 7.83%, 1.98%, and 0.86% respectively.

To summarize, we note that this section has shown that our scheme can achieve accurate results with a small N_k. With $N_k \sim 150$, the deviations $\Delta E/W \sim 10^{-3}$, $\langle|\Delta g/g|\rangle \sim 0.5\%$, and $\langle|\Delta\Phi/\Phi|\rangle \sim 0.1\%$ are within both experimental and theoretical uncertainties. These results are superior to those from other schemes with a much larger N_k.

V. APPLICATION TO REAL CRYSTALS

A. Band crossing and band switching

So far we have only considered the case of a single band. In real crystals, particularly for the electronic structure, we have complicated multiple bands and there is a new difficulty arising from band crossing and band switching. To be more specific, let us consider the first six bands[44] of Cu shown in Fig. 5. In each part of the figure, the bands are plotted as a function of k starting from the center of the BZ, Γ, and ending at a point on the XWU face as indicated by the dot in the separate picture above the bands. The circles are the first principle energies and the solid curves are obtained by connecting lines between 200 energies interpolated from the circles with Lagrange's formula. The coordinates (α, β, γ) are defined according to Eq. (4) with $\vec{q}_1 = \Gamma X$, $\vec{q}_2 = XW$, and $\vec{q}_3 = WU$. A comparison between Figs. 5(a) and 5(b) shows several changes: The degenerate Δ_5 band splits into two bands and complicated band switchings occur. The most noticeable is that the Δ_2 band crosses the upper Δ_1 band in Fig. 5(a) but the two bands switch to one another in Fig. 5(b). Band switching also occurs between Figs. 5(b) and 5(c). Thus, if the bands are labeled according to the smooth curves (i.e., according to the symmetry) along the Δ axis, some of them become discontinuous off the Δ axis. On the other hand, if bands are labeled according to the ordering in the energy, they have cusps and corners along the symmetry axes and on the symmetry planes as shown in Figs. 5(a) and 5(b). As Janak[23] pointed out, this problem of band crossing and band switching is the root of difficulties in the BZ interpolation for real crystals.

TABLE II. The average absolute percentage deviations (in %) for the calculated density of states, $\langle|\Delta g/g|\rangle$, and for the integrated density of states, $\langle|\Delta\Phi/\Phi|\rangle$, from the direct integration scheme (direct) and the ray integration (ray) for three sets of interpolation grids. The average is computed from those energies corresponding to the circles in Figs. 3(a)–4(c).

				$\langle\lvert\Delta g/g\rvert\rangle$			$\langle\lvert\Delta\Phi/\Phi\rvert\rangle$		
Method	N_A	N_B	N_C	sc	bcc	fcc	sc	bcc	fcc
direct	6	4	4	0.90	2.92	0.56	0.21	0.49	0.13
direct	6	5	5	0.71	1.60	0.62	0.07	0.12	0.18
direct	6	6	6	0.58	1.51	0.61	0.04	0.07	0.18
ray	6	4	4	0.81	2.90	0.40	0.21	0.51	0.13
ray	6	5	5	0.68	1.09	0.35	0.07	0.12	0.18
ray	6	6	6	0.58	0.59	0.33	0.09	0.06	0.13

However, we note that the band switching occurs only when the symmetry characters of the two $\vec{k}$ directions under consideration are different and the band crossing causes troubles only on the symmetry axes and on the symmetry planes. In other words, these problems do not happen in the general $\vec{k}$ directions. Although bands do contact at the general $\vec{k}$ points, as Herring[45] showed that they do, the occurrence is rare and even if they do the bands are smooth (having continuous gradients) and can be properly labeled according to the ordering in energies.

In this connection, we recall that our ray scheme has converted the BZ integrations into those along the axes of the thin tetrahedrons (the rays). All these rays are in the general $\vec{k}$ directions and never cross any symmetry planes except that the end points fall on the zone surface. Thus, if band quantities are available at the N_A grids $\{\alpha_i\}$ along the rays, they can be labeled according to the ordering in energies and the interpolation and integration can be carried out in a straightforward manner. The remaining question is how to obtain

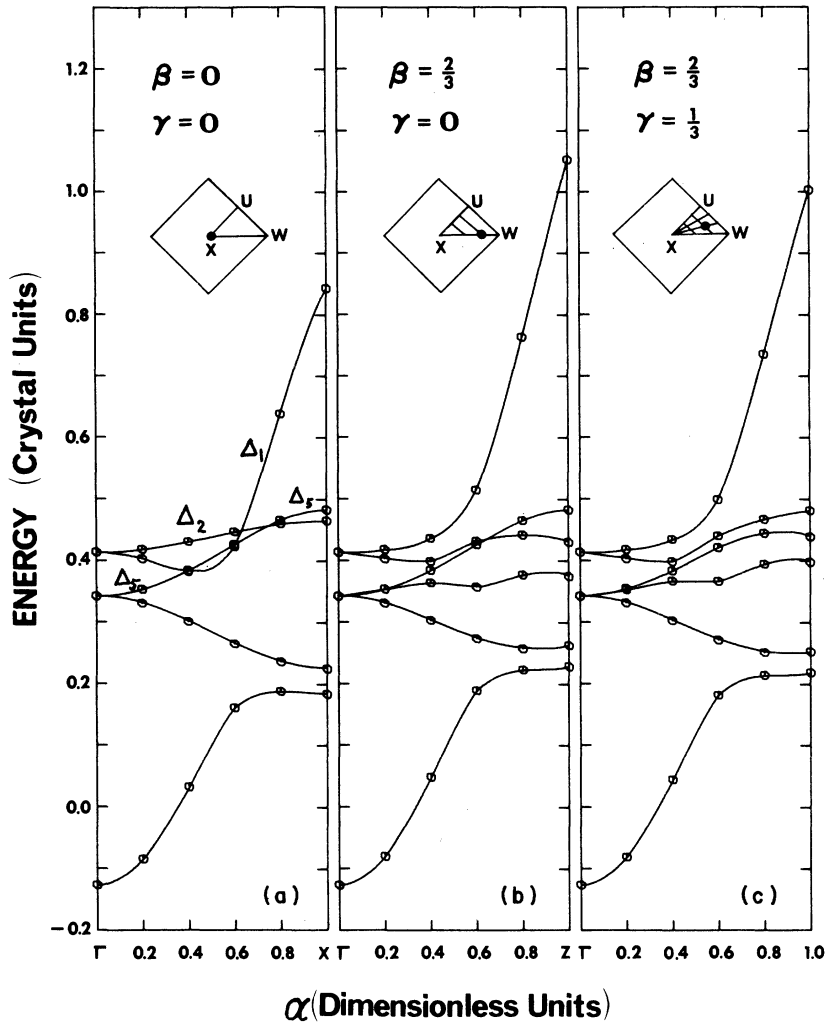

FIG. 5. Cu energy bands based on the Chodorow potential (Ref. 44) as a function of $\vec{k}$ from the center of the BZ, Γ, to the three $\vec{k}$ points on the *XWU* surface as indicated by the dots in the separate pictures. The circles are the energies calculated on the first-principles grid and the solid curves are the interpolated results from the circles using Lagrange's formula.

these quantities at these $\{\alpha_i\}$ from the first-principles grid.

We also recall that any $\vec{k}$-dependent function in a ray in terms of (α,β,γ) is a function of α only and has the values of β and γ fixed. So our problem is to obtain the $E_n(\alpha_i,\beta,\gamma)$ at α_i with i from 1 to N_A. According to Eq. (6), we have

$$E_n(\alpha_i,\beta,\gamma)=\sum_j\sum_m L_j(\beta)L_m(\gamma)E_n(\alpha_i,\beta_j,\gamma_m)\,. \tag{18}$$

For $i\neq N_A$ the band index n can be taken as that labeling the order of energy. For $i=N_A$ ($\alpha_i=1$) the $\vec{k}$ usually falls on a symmetry plane and we need to treat it as a special case. This special case can be handled easily: First, we label the first-principles bands for $\alpha=1$ according to their symmetry characters. Then, we apply Eq. (18) to obtain the E for the end point of each ray. Finally, we rearrange the band indices according to the ordering in energies before we apply the ray integration. Since the special case can be handled very easily with our coordinate system, our scheme can now be applied to real crystals.

B. Density of states for Cu

To demonstrate the applicability of the above procedures, we have calculated the density of states $g(E)$ for Cu. The first-principles $E_n(\vec{k})$ were calculated using the Chodorow potential[44] in the KKR method with a maximum angular momentum $l=2$. The first-principles grid used corresponds to $N_A=6$ and $N_B=N_C=4$ (i.e., $N_k=147$). The integration mesh used is the same as that in Sec. IV. The $g(E)$ were calculated at an energy mesh corresponding to an interval of 0.03 eV. Straight lines are connected between two successive calculated $g(E_i)$ to give the curve in Fig. 6. The quality of the calculation can be seen from

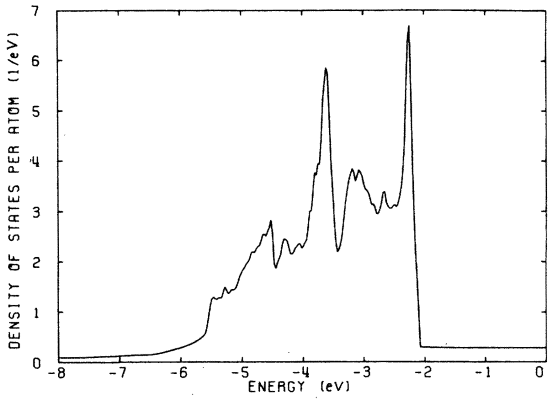

FIG. 6. Density of states of Cu calculated from the ray integration using the interpolation procedures described in Sec. V. The energy bands used in the calculations are the same as those shown in Fig. 5.

the smoothness of the curve below and above the d band. The general feature of the $g(E)$ and the strengths of the major peaks are in agreement with the published Cu density of states.[46] We feel that the curve shown in Fig. 6 represents the true spectra for the band structure considered.

VI. SUMMARY AND DISCUSSION

This work is a result of search for a simple and accurate BZ interpolation and integration package. The main feature in this work is the utilization of a system of convenient coordinates (α,β,γ) which allows systematic application of one-dimensional numerical procedures in the interpolation and integration. The difficult problem associated with the band crossing and band switching in real crystals can also be handled easily within our scheme. In its first trial, the scheme has produced very good results for the tight-binding band models and for the density of states of Cu. Therefore, our objective to produce good spectra using a small number of first-principles $\vec{k}$ points has been accomplished. With its simplicity, accuracy, and uniformity, the present scheme should be attractive to workers interested in calculating the spectral properties, particularly in the angular dependent spectra.

It should be pointed out that the present approach is connected with previous schemes and has incorporated many of their good features. One idea which is common between the original tetrahedron[28] schemes and our ray integration is that the microzones used fill up the volume of the BZ exactly. Another common advantage is that both approaches do not require the calculation of the energy gradients $\nabla_k E(\vec{k})$ on the first-principles grid. Our concept of using the rays in the nonrectangular coordinates resembles the idea used in the constant energy search routine in the KKR method developed by Faulkner *et al.*[47] and improved by Butler *et al.*[48] However, our idea of using the one-dimensional integration was originally motivated by Bansil's[10] work on the special directions in the BZ. In that work, Bansil optimized the ray integrations in a small number of "special directions" to represent the integrated function. This technique is similar to that in the "special points" in the BZ used by Chadi and Cohen[49] for smoothly varying functions of $\vec{k}$. It may be possible to use Bansil's approach by choosing special directions for special cases, but as a general scheme his approach is not expected to be accurate. One important reason for this is that the angular dependence of the ray integrals often varies very violently (e.g., constant energy surfaces in pure crystals usually have cusps and discontinuities) and the variations are different for different functions. Clearly a remedy for this approach is to include a sufficiently large number of rays. This point has been demonstrated in our test in Sec. IV and in a work by Overton and Schuch,[50] who employed a more elaborate one-dimensional integration scheme with a mesh corresponding to using 105 $\vec{k}$ points for each of 489 rays (i.e., $N_k = 51345$) to achieve highly accurate phonon density of states and the Debye Θ. This and earlier (Sec. I) considerations clearly bear out the importance of the interpolation scheme. Thus we can say that our greatest accomplishment in this work is to have obtained a simple interpolation scheme which enables us to incorporate the ray integrals in real application.

Although we have only demonstrated the applicability of our scheme in pure crystals, we expect that the technique can be extended to deal with impurities[4,5] and disordered alloys.[6-13] In the scattering formalism for these systems,[4-13] the important and difficult part of the calculation is the BZ integration with the appropriate Green's functions as the integrands. In addition to the expressions like Eq. (2), the principal parts of Green's functions have to be evaluated. For alloys, there is a further complication which arises from the fact that the poles of the alloy Green's function are complex numbers[11] so that the spectral density functions are not the δ function but are spiky functions with finite widths.[11,13] To evaluate these integrals, it is important to locate the poles of the Green's function or the peaks of the spectral density functions, which can be handled with our interpolation method. There is another problem which is associated with the singularities of the free-election Green's function, but a treatment of that problem has already been studied.[51] Thus, with the ability to locate the singular structures of

the integrands, we expect that a systematic and efficient treatment of these functions can be achieved with the one-dimensional ray integrations. Hopeful signs related to the above have been found in the recent studies of the alloy electronic structure based on the muffin-tin potentials using the average-t-matrix approximation[11] and the coherent potential approximation.[13]

Finally, we note that here we have presented the results for the first trial of our scheme and we expect that further improvements can be made in different aspects of its application. For example, an improvement in the accuracy may be achievable by subdividing the thin tetrahedrons used in the ray integration into microtetrahedrons in which the original tetrahedron integration results[28] can be used. The accuracy can also be improved if the energy gradients $\nabla_k E$ are also included in the calculations. However, improvements as such represent a fine tuning for the application. The present scheme as it stands is already accurate and efficient enough for vast applications. We plan to couple the present scheme with the GFM parametrization scheme[17] mentioned earlier for a systematic empirical parametrization of the electronic structure of metals. We believe that such a systematic correlation between the band structures and the experimental data in metals can improve our present understanding of the electronic structures and the fundamental processes in crystals, which in turn can provide a better basis for the study of more complex systems such as impurities, disordered alloys and surfaces, etc.

ACKNOWLEDGMENT

I wish to thank Professor B. Segall for informative discussions.

---

*Partially supported by a grant from the Auburn University Grant-in-Aid Program.

[1]For a review of this topic, see Refs. 2 and 3, and the references therein.
[2]G. Gilat, Methods Comput. Phys. 15, 317 (1976).
[3]G. Gilat, J. Comp. Phys. 10, 432 (1972).
[4]K. H. Johnson and F. C. Smith, Jr., in *Computational Method in Band Theory*, edited by P. O. Marcus, J. F. Janak, and A. R. Williams (Plenum, New York, 1971), p. 377 and references therein.
[5]R. H. Lasseter and P. Soven, Phys. Rev. B 8, 2476 (1973).
[6]P. Soven, Phys. Rev. B 2, 4715 (1970).
[7]B. L. Gyorffy, Phys. Rev. B 5, 2382 (1972).
[8]A.-B. Chen, Phys. Rev. B 7, 2230 (1973).
[9]L. Schwartz and A. Bansil, Phys. Rev. B 10, 3261 (1974).
[10]A. Bansil, Solid State Commun. 16, 885 (1975).
[11]A. Bansil, L. M. Schwartz, and H. Ehrenreich, Phys. Rev. B 12, 2893 (1975).
[12]H. Ehrenreich and L. M. Schwartz, Solid State Phys. 31, 150 (1976).
[13]G. M. Stocks, B. L. Gyorffy, and W. E. Temmerman, Bull. Am. Phys. Soc. 22, 348 (1977).
[14]B. Segall and F. S. Ham, Methods Comput. Phys. 8, 251 (1968).
[15]W. Kohn and N. Rostoker, Phys. Rev. 94, 1111 (1954).
[16]J. Korringa, Physica (Utr.) 13, 392 (1947).
[17]A.-B. Chen and B. Segall, Phys. Rev. B 12, 600 (1965).
[18]A.- B. Chen and B. Segall (unpublished).
[19]M. Blackman, Proc. R. Phys. Soc. (Lond.) A159, 416 (1937).
[20]D. Brust, Phys. Rev. 139, A489 (1965) and Methods Comput. Phys. 8, 33 (1968).
[21]G. Gilat and G. Dolling, Phys. Lett. 22, 715 (1964).
[22]G. Gilat and L. J. Raubenheimer, Phys. Rev. 144, 390 (1966).
[23]J. F. Janak, in *Computational Methods in Band Theory*, edited by P. M. Marcus, J. F. Janak, and A. R. Williams (Plenum, New York, 1971), p. 323.
[24]F. M. Mueller, J. W. Garland, M. H. Cohen, and K. H. Benneman, Ann. Phys. (N.Y.) 67, 19 (1971).
[25]F. M. Mueller, in *Computational Methods in Band Theory*, edited by P. M. Marcus, J. F. Janak, and A. R. Williams (Plenum, New York, 1971), p. 305.
[26]J. F. Janak, D. E. Eastman, and A. R. Williams, Solid State Commun. 8, 271 (1970).
[27]J. F. Cooke and R. F. Wood, Phys. Rev. B 5, 1276 (1972).
[28]J. Rath and A. J. Freeman, Phys. Rev. B 11, 2109 (1975) and references therein.
[29]P. A. Lingård, Solid State Commun. 16, 481 (1975).
[30]G. Gilat and F. Herman, Ann. Phys. (N.Y.) 67, 432 (1971).
[31]L. Hodges, H. Ehrenreich, and N. D. Lang, Phys. Rev. 152, 505 (1966).
[32]F. Mueller, Phys. Rev. 153, 659 (1967).
[33]J. W. D. Connolly, in *Electronic Density of States*, Natl. Bur. Stand. Special Pub. No. 332, edited by L. H. Bennett (U.S. GPO, Washington, D.C., 1971), p. 27.
[34]C. Y. Fong and M. L. Cohen, Phys. Rev. Lett. 24, 306 (1970).
[35]N. V. Smith and L. F. Mattheiss, Phys. Rev. B 9, 1341 (1974).
[36]J. F. Janak, A. R. Williams, and V. L. Moruzzi, Phys. Rev. B 11, 1522 (1975).
[37]R. J. Jelitto, Phys. Chem. Solids 30, 609 (1969).
[38]A. W. Luehrmann, Adv. Phys. 17, 1 (1968), where the Brillouin zones for all the symmorphic space groups are available and are analyzed.
[39]See, for example, *Handbook of Mathematical Functions*, 10th ed., edited by M. Abramowitz and I. A. Stegun (Nat. Bur. Stand. Appl. Math. Series. 55, 1972), p. 886.
[40]The exact $\Phi(E)$ are obtained from integrating the expressions $g(E)$ given by Eqs. 39(a) to 39(c) in Ref. 37.
[41]See Fig. 3 of Ref. 2.
[42]J. F. Janak, D. E. Eastman, and A. R. Williams, in

Electronic Density of States, edited by L. H. Bennett (Natl. Bur. Stand. Spec. Pub. 323, 1971), p. 181.
[43]E. B. Kennard, D. Koskimaki, J. T. Waber, and F. M. Mueller, *In Electronic Density of States*, edited by L. H. Bennett (Natl. Bur. Stand. Spec. Pub. 323, 1971), p. 795.
[44]The same Cu potential used by B. Segall, Phys. Rev. 125, 109 (1962) and by G. A. Burdick, Phys. Rev. 129, 138 (1963) but with a lattice constant of 6.8090 a.u.
[45]C. Herring, Phys. Rev. 52, 365 (1937).
[46]See, for example, see Fig. 7 of Ref. 32, Fig. 1 of Ref. 42, and N. V. Smith, Phys. Rev. B 3, 1862 (1971), Fig. 19.
and N. V. Smith, Phys. Rev. B 3, 1862 (1971), Fig. 19.
[47]J. S. Faulkner, H. L. Davis, and H. W. Joy, Phys. Rev. 161, 656 (1967).
[48]W.H. Butler, J. J. Olson, J. S. Faulkner, and B. L. Gyorffy, Phys. Rev. B 14, 3823 (1976).
[49]D. J. Chadi and M. L. Cohen, Phys. Rev. B 8, 5747 (1973).
[50]W. C. Overton, Jr., and A. F. Schuch, J. Comp. Phys. 14, 59 (1974).
[51]B. Segall and A.-B. Chen, Phys. Rev. B 16, 2556 (1977).